23rd International Workshop on Laser Ranging
Kunming, China, 20-26 October 2024

Scientific Applications of Satellite Laser Ranging

Testing Local Lorentz Invariance with SLR

David Lucchesi[(1,2,3)], Massimo Visco[(1,2)], **Roberto Peron**[(1,2)], Giuseppe Pucacco[(2,4)], Luciano Anselmo[(3)], Massimo Bassan[(2,4)], Marco Cinelli[(1,2)], Alessandro Di Marco[(1,2)], Marco Lucente[(1,2)], Carmelo Magnafico[(1,2)], Carmen Pardini[(3)], Josè Rodriguez[(5)], Feliciana Sapio[(1,2)]

(1) Istituto di Astrofisica e Planetologia Spaziali (IAPS) – Istituto Nazionale di Astrofisica (INAF), Tor Vergata - Roma, Italy

(2) Istituto Nazionale di Fisica Nucleare (INFN), Tor Vergata - Roma, Italy

(3) Istituto di Scienza e Tecnologie dell'Informazione (ISTI) – Consiglio Nazionale delle Ricerche (CNR). Pisa, Italy

Dipartimento di Fisica – Università di Tor Vergata, Tor Vergata - Roma, Italy

Instituto Geografico National (IGN), Madrid, Spain

david.lucchesi@inaf.it

roberto.peron@inaf.it

Local Lorentz Invariance

One way to look for evidence of *new physics* beyond **Special Relativity** (**SR**) and **General Relativity** (**GR**) is to check for violations, apparent or effective, of the pillars of Einstein's theories.

For example, **Lorentz invariance** is a feature of both **SR** and **GR**.

The fusion of **Special Relativity** with **Quantum Mechanics** was very successful in the development of **Quantum Field Theory** and, ultimately, the current **Standard Model** of particles and fields.

However, violations of **Lorentz invariance** could arise from some models of **Quantum Gravity** (**QG**). Indeed, the **Planck length** represents a fundamental length scale in **QG**, but it is not an invariant quantity: **Lorentz invariance** might be violated at some level.

$$L_P = \sqrt{\frac{hG}{2\pi c^3}} \cong 2 \times 10^{-33}\ \mathrm{cm}$$

Local Lorentz Invariance

Local Lorentz Invariance (**LLI**) states that the outcome of any **local** (in space and time) non-gravitational experiment is **independent** of the **velocity** of the **freely-falling** reference frame in which the experiment is performed.

Modern unification theories suggest that the gravitational long-range interaction between macroscopic bodies may be mediated, not only by the metric tensor field $\mathbf{g}_{\mu\nu}$ of **GR** but also by other fields (**scalar**, **vector**, or **tensor**).

More generally, besides **GR**, any metrically coupled **tensor-scalar** theory of gravitation does not predict **any violation** of **local boost invariance**. This is for example the case of the **Brans-Dicke** theory of gravitation which includes the existence of a scalar field ϕ.

Local Lorentz Invariance is a key ingredient of the
(**Einstein** or **Strong**) **Equivalence Principle**

Local Lorentz Invariance

However, in the case of theories that contain **vector fields** or other **tensor fields** in addition to the metric tensor $\mathbf{g}_{\mu\nu}$, one expects that the **global distribution of matter** in the **Universe** select a <u>**preferred rest frame**</u> for the local gravitational interaction.

In this case the **physical laws** could be **different** from a **moving observer** with respect to a **stationary one**, also considering their relative orientation...

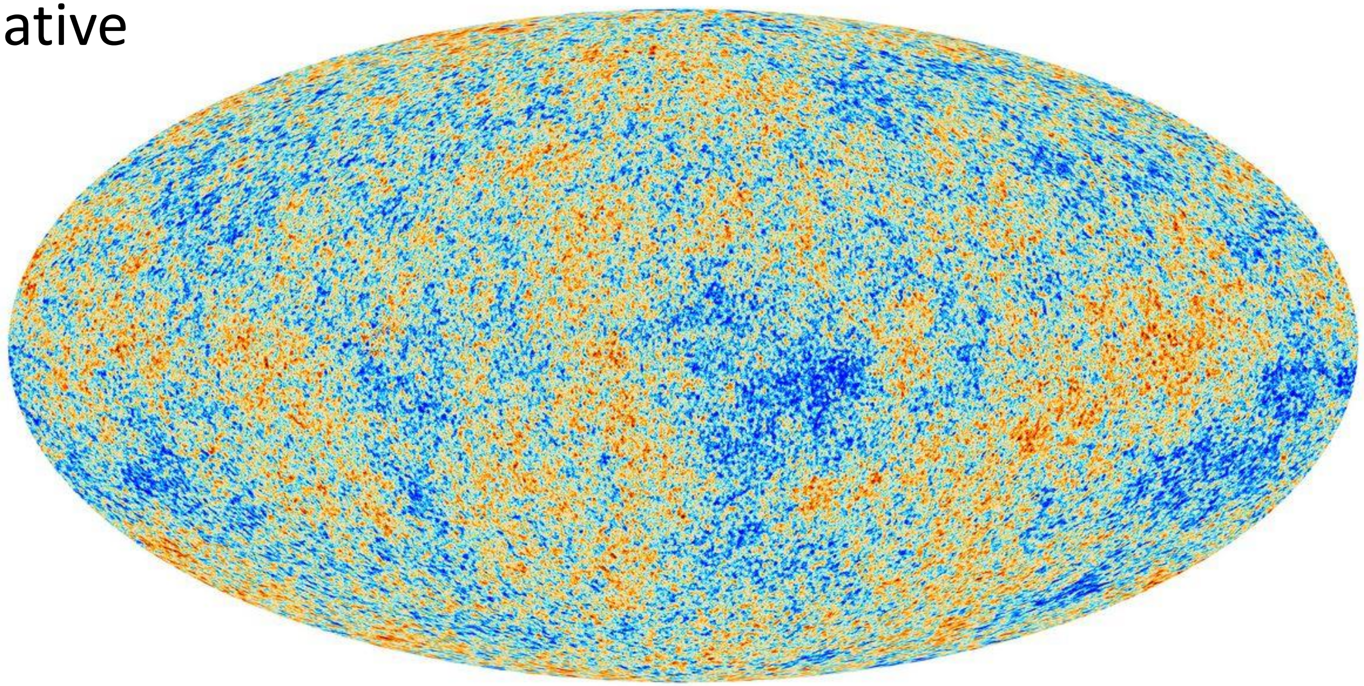

Credits: ESA and Planck collaboration

Summarizing:

In **theories** of gravity with $\begin{cases} g_{\mu\nu} \\ \phi \end{cases}$ **LLI holds,**

while in **theories** with $\begin{cases} g_{\mu\nu} \\ K^{\mu} \end{cases}$

or with $\begin{cases} g_{\mu\nu} \\ C_{\mu\nu} \end{cases}$ **LLI** is violated.

Local Lorentz Invariance

SaToR-G

Nordtvedt, K. *Equivalence Principle for Massive Bodies. II. Theory*. Phys. Rev. **1968**, 169, 1017–1025
Will, C.M. *Theoretical Frameworks for Testing Relativistic Gravity. II. Parametrized Post-Newtonian Hydrodynamics, and the Nordtvedt Effect*. Astrophys. J. **1971**, 163, 611–628
Will, C.M.; Nordtvedt, J.K. *Conservation Laws and Preferred Frames in Relativistic Gravity. I. Preferred-Frame Theories and an Extended PPN Formalism*. Astrophys. J. **1972**, 177, 757–774

The parameterized post-Newtonian (PPN) formalism

- One way to test a theory of gravitation is by studying its post-Newtonian limit
- Post-Newtonian formalism or **PPN** formalism details the parameters in which different metric theories of gravity, under **weak-field** and **slow-motion** (**WFSM**) conditions, can differ from Newtonian gravity

$$
\begin{aligned}
g_{00} = & -1 + 2U - 2\beta U^2 - 2\xi\Phi_W + (2\gamma + 2 + \alpha_3 + \zeta_1 - 2\xi)\Phi_1 + 2(3\gamma - 2\beta + 1 + \zeta_2 + \xi)\Phi_2 \\
& + 2(1+\zeta_3)\Phi_3 + 2(3\gamma + 3\zeta_4 - 2\xi)\Phi_4 - (\zeta_1 - 2\xi)\mathcal{A} - (\alpha_1 - \alpha_2 - \alpha_3)w^2 U - \alpha_2 w^i w^j U_{ij} \\
& + (2\alpha_3 - \alpha_1)w^i V_i + \mathcal{O}(\epsilon^3), \\
g_{0i} = & -\frac{1}{2}(4\gamma + 3 + \alpha_1 - \alpha_2 + \zeta_1 - 2\xi)V_i - \frac{1}{2}(1 + \alpha_2 - \zeta_1 + 2\xi)W_i - \frac{1}{2}(\alpha_1 - 2\alpha_2)w^i U \\
& - \alpha_2 w^j U_{ij} + \mathcal{O}(\epsilon^{5/2}), \\
g_{ij} = & (1 + 2\gamma U)\delta_{ij} + \mathcal{O}(\epsilon^2).
\end{aligned}
$$

Metric

$$
\begin{aligned}
T^{00} &= \rho(1 + \Pi + v^2 + 2U), \\
T^{0i} &= \rho v^i \left(1 + \Pi + v^2 + 2U + \frac{p}{\rho}\right), \\
T^{ij} &= \rho v^i v^j \left(1 + \Pi + v^2 + 2U + \frac{p}{\rho}\right) + p\delta^{ij}(1 - 2\gamma U).
\end{aligned}
$$

Stress-Energy Tensor

C.M. Will *Living Rev. Relativity*, 17, (2014), 4

$$
\begin{aligned}
U &= \int \frac{\rho'}{|\mathbf{x}-\mathbf{x}'|}\, d^3x', \\
U_{ij} &= \int \frac{\rho'(x-x')_i(x-x')_j}{|\mathbf{x}-\mathbf{x}'|^3}\, d^3x', \\
\Phi_W &= \int \frac{\rho'\rho''(\mathbf{x}-\mathbf{x}')}{|\mathbf{x}-\mathbf{x}'|^3} \cdot \left(\frac{\mathbf{x}'-\mathbf{x}''}{|\mathbf{x}-\mathbf{x}''|} - \frac{\mathbf{x}-\mathbf{x}''}{|\mathbf{x}'-\mathbf{x}''|}\right) d^3x'\, d^3x'', \\
\mathcal{A} &= \int \frac{\rho'[\mathbf{v}'\cdot(\mathbf{x}-\mathbf{x}')]^2}{|\mathbf{x}-\mathbf{x}'|^3}\, d^3x', \\
\Phi_1 &= \int \frac{\rho' v'^2}{|\mathbf{x}-\mathbf{x}'|}\, d^3x', \\
\Phi_2 &= \int \frac{\rho' U'}{|\mathbf{x}-\mathbf{x}'|}\, d^3x', \\
\Phi_3 &= \int \frac{\rho'\Pi'}{|\mathbf{x}-\mathbf{x}'|}\, d^3x', \\
\Phi_4 &= \int \frac{p'}{|\mathbf{x}-\mathbf{x}'|}\, d^3x', \\
V_i &= \int \frac{\rho' v'_i}{|\mathbf{x}-\mathbf{x}'|}\, d^3x', \\
W_i &= \int \frac{\rho'[\mathbf{v}'\cdot(\mathbf{x}-\mathbf{x}')](x-x')_i}{|\mathbf{x}-\mathbf{x}'|^3}\, d^3x'.
\end{aligned}
$$

Metric Potentials

Local Lorentz Invariance

From the phenomenological point of view, and in the framework of the **parameterized post-Newtonian** (**PPN**) formalism [1,2,3], valid in the **WFSM** limit of **GR**, the **Preferred Frame Effects** (**PFE**) are described by the parameters $\boldsymbol{\alpha_1}$, $\boldsymbol{\alpha_2}$ and $\boldsymbol{\alpha_3}$, all equal to zero in **GR** and in tensor-scalar theories of gravitation.

In particular, in the case of the interaction of **N** masses, the **Lagrangian** depends on the two parameters $\boldsymbol{\alpha_1}$ and $\boldsymbol{\alpha_2}$, that, <u>if different from zero</u>, will provide <u>non-boost invariant terms</u> depending on the **velocities** ($\boldsymbol{v}_a^0$) of the test masses with respect to some **gravitationally preferred rest frame** [4]:

$$\mathcal{L}^N = \mathcal{L}_{\beta,\gamma,\eta} + \mathcal{L}_{\alpha_1} + \mathcal{L}_{\alpha_2}$$

$$\mathcal{L}_{\alpha_1} = -\frac{\alpha_1}{4c^2}\sum_{a\neq b}\frac{G m_a m_b}{r_{ab}}\left(\boldsymbol{v}_a^0 \cdot \boldsymbol{v}_b^0\right)$$

1. **Nordtvedt, K.** *Equivalence Principle for Massive Bodies. II. Theory*. Phys. Rev. **1968**, 169, 1017–1025
2. **Will, C.M.** *Theoretical Frameworks for Testing Relativistic Gravity. II. Parametrized Post-Newtonian Hydrodynamics, and the Nordtvedt Effect*. Astrophys. J. **1971**, 163, 611–628
3. **Will, C.M.; Nordtvedt, K.** *Conservation Laws and Preferred Frames in Relativistic Gravity. I. Preferred-Frame Theories and an Extended PPN Formalism*. Astrophys. J. **1972**, 177, 757–774
4. **Damour, T.; Esposito-Farese. G**. *Testing for preferred-frame effects in gravity with artificial Earth satellites*. Phys. Rev. D **1994**, 49, 4, 1693-1706

Local Lorentz Invariance

LLI and, consequently, **PFE**, are **well tested** in the context of **high-energy physics experiments** but are **much more difficult** to test in the context of **gravitation**, both in the **weak-field** regime and in the **strong-** or **quasi-strong-field** regime.

Living Rev. Relativity, **8**, (2005), 5
http://www.livingreviews.org/lrr-2005-5

Modern Tests of Lorentz Invariance

David Mattingly
Department of Physics
University of California at Davis
Davis, CA 95616, U.S.A.
email: mattingly@physics.ucdavis.edu
http://lifshitz.ucdavis.edu/~mattingly

Accepted on 4 July 2005
Published on 7 September 2005

Living Reviews in Relativity
Published by the
Max Planck Institute for Gravitational Physics
(Albert Einstein Institute)
Am Mühlenberg 1, 14424 Golm, Germany
ISSN 1433-8351

Abstract

Motivated by ideas about quantum gravity, a tremendous amount of effort over the past decade has gone into testing Lorentz invariance in various regimes. This review summarizes both the theoretical frameworks for tests of Lorentz invariance and experimental advances that have made new high precision tests possible. The current constraints on Lorentz violating effects from both terrestrial experiments and astrophysical observations are presented.

IOP Publishing — Classical and Quantum Gravity
Class. Quantum Grav. **30** (2013) 133001 (50pp) doi:10.1088/0264-9381/30/13/133001

TOPICAL REVIEW

Tests of Lorentz invariance: a 2013 update

S Liberati

SISSA, Via Bonomea 265, I-34136 Trieste, Italy
INFN, Via Valerio 2, I-34100 Trieste, Italy

E-mail: liberati@sissa.it

Received 28 February 2013, in final form 22 March 2013
Published 7 June 2013
Online at stacks.iop.org/CQG/30/133001

Abstract
We present an updated review of Lorentz invariance tests in effective field theories (EFTs) in the matter as well as in the gravity sector. After a general discussion of the role of Lorentz invariance and a derivation of its transformations along the so-called von Ignatovski theorem, we present the dynamical frameworks developed within local EFT and the available constraints on the parameters governing the Lorentz breaking effects. In the end, we discuss two specific examples: the OPERA 'affaire' and the case of Hořava–Lifshitz gravity. The first case will serve as an example, and a caveat, of the practical application of the general techniques developed for constraining Lorentz invariance violation to a direct observation potentially showing these effects. The second case will show how the application of the same techniques to a specific quantum gravity scenario has far-reaching implications not foreseeable in a purely phenomenological EFT approach.

PACS numbers: 98.70.Rz, 04.60.−m, 11.30.Cp, 12.20.Fv

Local Lorentz Invariance

In 1994, **Damour** and **Esposito-Farese** have shown that the orbits of some **artificial satellites** have the potential to provide improvements in the **limit** of the α_1 parameter down to the $\mathbf{10^{-6}}$ level, thanks to the appearance of **small divisors** which enhance the corresponding **PFE**.

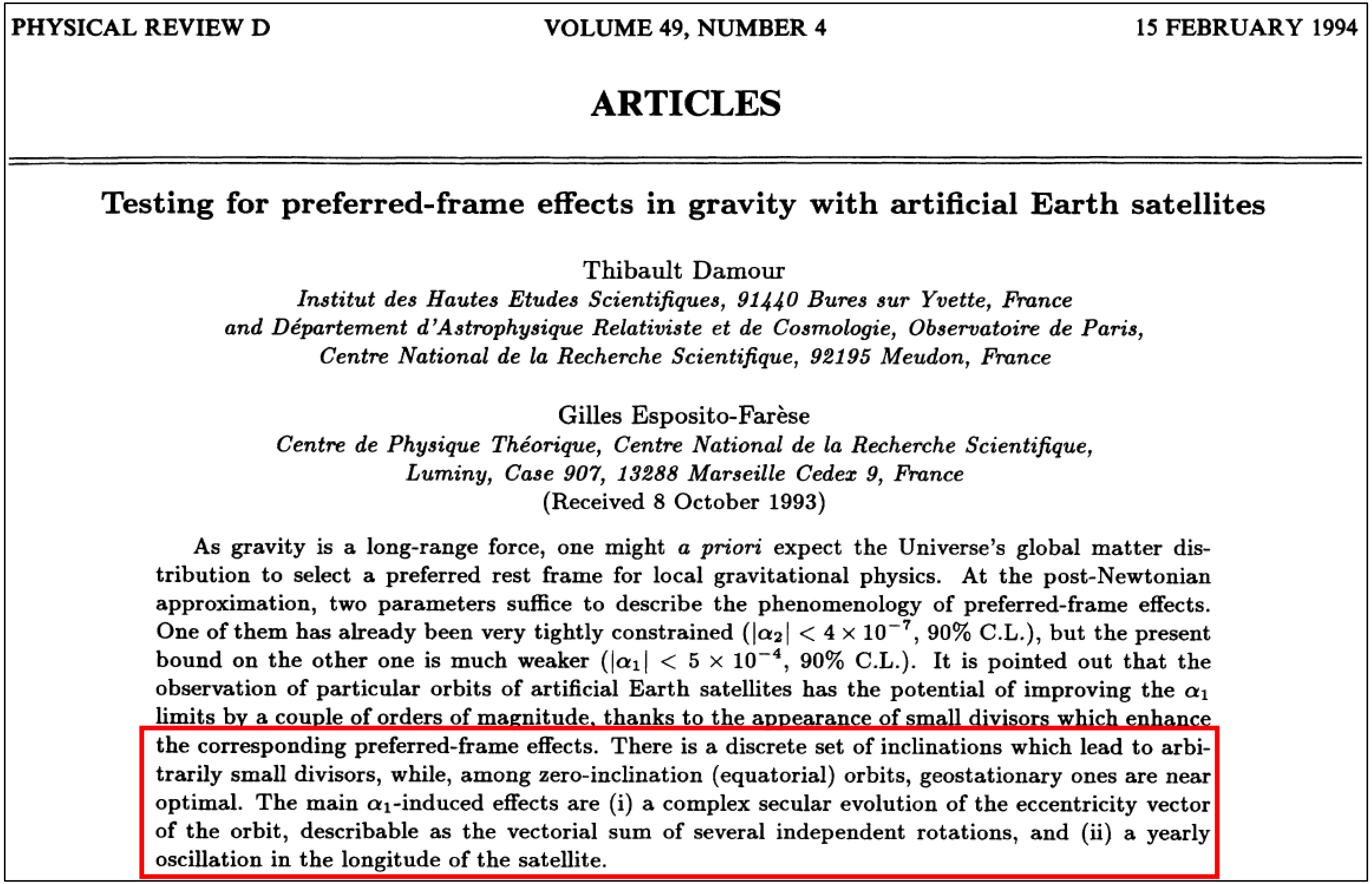

PHYSICAL REVIEW D VOLUME 49, NUMBER 4 15 FEBRUARY 1994

ARTICLES

Testing for preferred-frame effects in gravity with artificial Earth satellites

Thibault Damour
Institut des Hautes Etudes Scientifiques, 91440 Bures sur Yvette, France
and Département d'Astrophysique Relativiste et de Cosmologie, Observatoire de Paris,
Centre National de la Recherche Scientifique, 92195 Meudon, France

Gilles Esposito-Farèse
Centre de Physique Théorique, Centre National de la Recherche Scientifique,
Luminy, Case 907, 13288 Marseille Cedex 9, France

(Received 8 October 1993)

As gravity is a long-range force, one might *a priori* expect the Universe's global matter distribution to select a preferred rest frame for local gravitational physics. At the post-Newtonian approximation, two parameters suffice to describe the phenomenology of preferred-frame effects. One of them has already been very tightly constrained ($|\alpha_2| < 4 \times 10^{-7}$, 90% C.L.), but the present bound on the other one is much weaker ($|\alpha_1| < 5 \times 10^{-4}$, 90% C.L.). It is pointed out that the observation of particular orbits of artificial Earth satellites has the potential of improving the α_1 limits by a couple of orders of magnitude, thanks to the appearance of small divisors which enhance the corresponding preferred-frame effects. There is a discrete set of inclinations which lead to arbitrarily small divisors, while, among zero-inclination (equatorial) orbits, geostationary ones are near optimal. The main α_1-induced effects are (i) a complex secular evolution of the eccentricity vector of the orbit, describable as the vectorial sum of several independent rotations, and (ii) a yearly oscillation in the longitude of the satellite.

The SaToR-G experiment

Satellite **T**ests **o**f **R**elativistic **G**ravity (**SaToR-G**, started on 2020) and the previous **LA**ser **RA**nged **S**atellites **E**xperiment (**LARASE**, 2013-2019) are two experiments devoted to measurements of the gravitational interaction in the **WFSM** limit of **GR** by means of laser tracking to geodetic passive satellites orbiting around the Earth. The two experiments were and are funded by the **Italian National Institute for Nuclear Physics** (**INFN-CSN2**).

In particular, **SaToR-G** aims to test gravitation beyond the predictions of **GR** searching for effects foreseen by **alternative theories of gravitation** (**ATG**) and possibly connected with ***"new physics".***

SaToR-G builds on the improved dynamical model of the two **LAGEOS** and **LARES** satellites achieved within the previous project **LARASE.**

The improvements concern the modeling of both **gravitational** and **non-gravitational perturbations**.

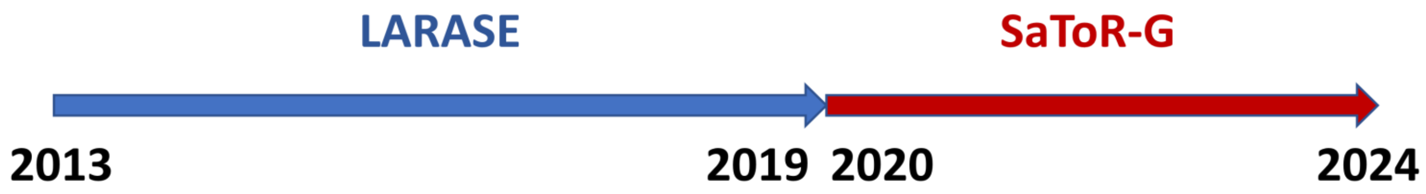

The SaToR-G experiment

From the analysis of **satellite orbits** it is possible to obtain a series of measurements of **gravitational effects** with consequent constraints on **different theories of gravitation**. The main ones include:

1. **Relativistic precessions**
2. **Constraints on long-range interactions**
3. **Nonlinearity of the gravitational interaction**
4. **Local Lorentz Invariance**
5. **Equivalence Principle**
6. **…**

From these measurements it is possible to obtain **constraints** on **PPN parameters** and their combinations.

The ultimate goal is to provide **precise** and **accurate measurements**, in the sense of a **robust** and **reliable evaluation** of **systematic errors**, in order to obtain **significant constraints** for the **different theories**.

The SaToR-G experiment

From these two main measurements:

1. Lense-Thirring precession of the nodes of LAGEOS, LAGEOS II and LARES
2. Relativistic precession of the argument of pericenter and mean anomaly of LAGEOS II (Schwarzschild, …)

$$\mu - 1 = (1.5 \pm 7.4) \times 10^{-3} \pm 16 \times 10^{-3}$$

$$\varepsilon - 1 = (-0.12 \pm 2.10) \times 10^{-3} \pm 2.5 \times 10^{-2}$$

we were already able to constrain the gravitational interaction for several physical theories of gravitation:

1. PPN parameters
2. Extended gravity theories
3. Yukawa-like long-range interactions
4. Torsional theories of gravity
5. Vector-tensor theories of gravity

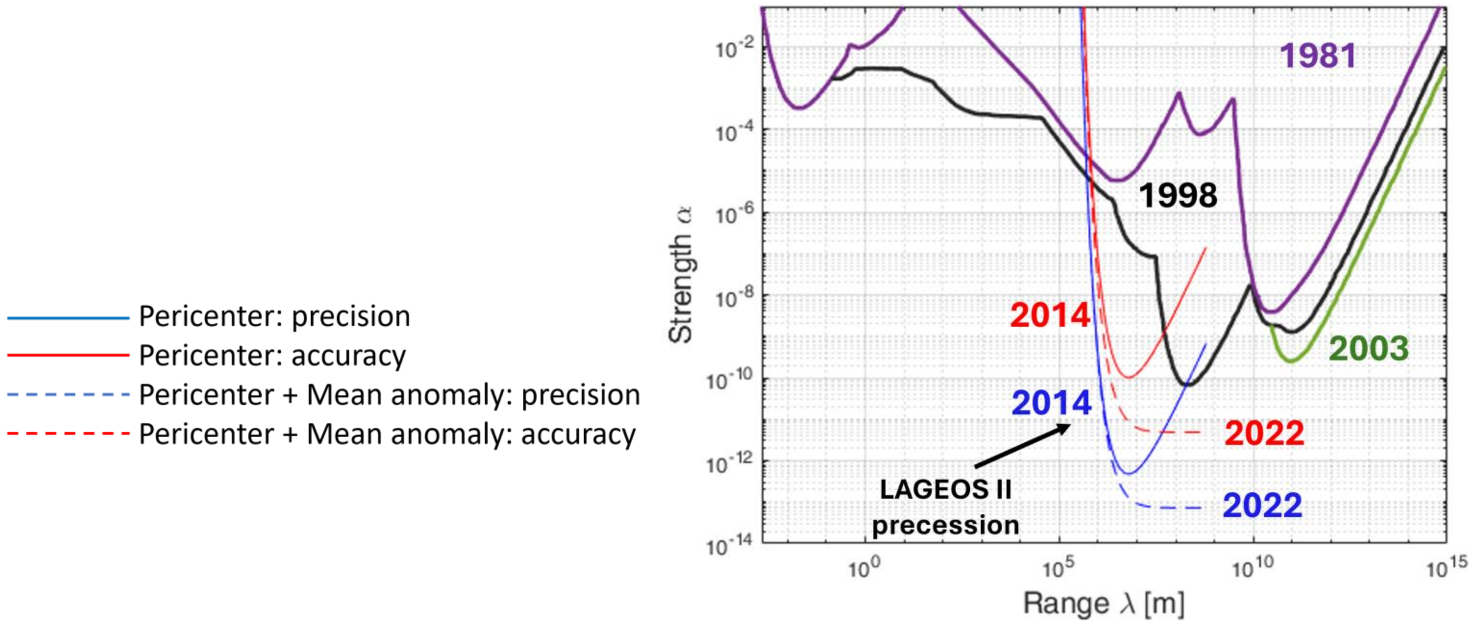

The test masses

The predictions of **GR** on the orbits of **geodetic satellites**, which play the role of **test masses**, are compared with those of **ATG** both **metric** and **non-metric** in their essence.

Parameter	Unit	Symbol	LAGEOS	LAGEOS II	LARES
Semi-major axis	km	a	12 270.00	12 162.08	7 820.31
Eccentricity	-	e	0.0044	0.0138	0.0012
Inclination	deg.	i	109.84	52.66	69.49
Radius	cm	R	30.0	30.0	18.2
Mass	kg	M	406.9	405.4	383.8
Area/Mass	m^2/kg	A/M	6.94×10^{-4}	6.97×10^{-4}	2.69×10^{-4}

LAGEOS (NASA, 1976)

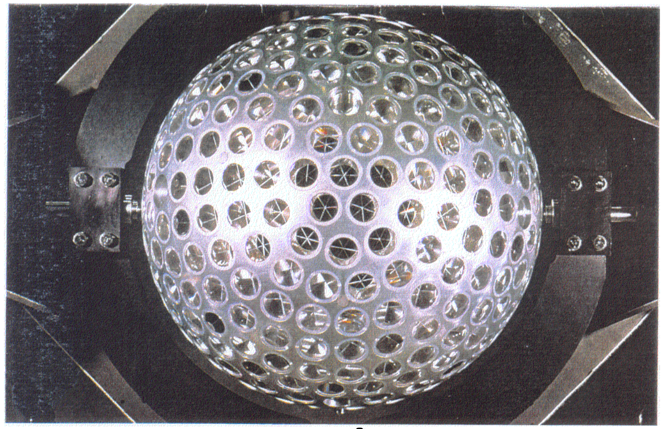

LAGEOS II (ASI/NASA, 1992)

LARES (ASI, 2012)

Precise Orbit Determination

Currently, we are using the following software in our **POD**:

- **GEODYN II** (NASA/GSFC)
- **SATAN** (NSGF, UK) in collaboration with “Observatorio de YEBES” (Spain) (under test)
- **Bernese** (University of Bern, CH)

1. From a least squares fit of the tracking data by means of an appropriate dynamic model, the estimate of the state vector of the satellite over 7-day arcs is obtained.

2. Then from an appropriate comparison between the state vector estimated at the beginning of each arc and the state vector estimated at the beginning of the previous arc but propagated at the same epoch, the residuals in the orbital elements are obtained: $\Delta\vec{x}_{res} = \vec{x}_{est} - \vec{x}_{pro}$.

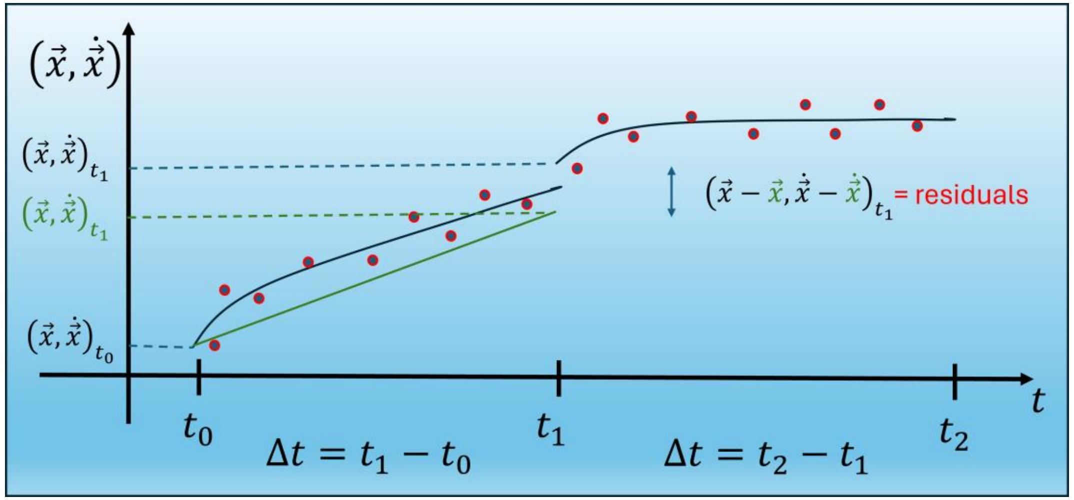

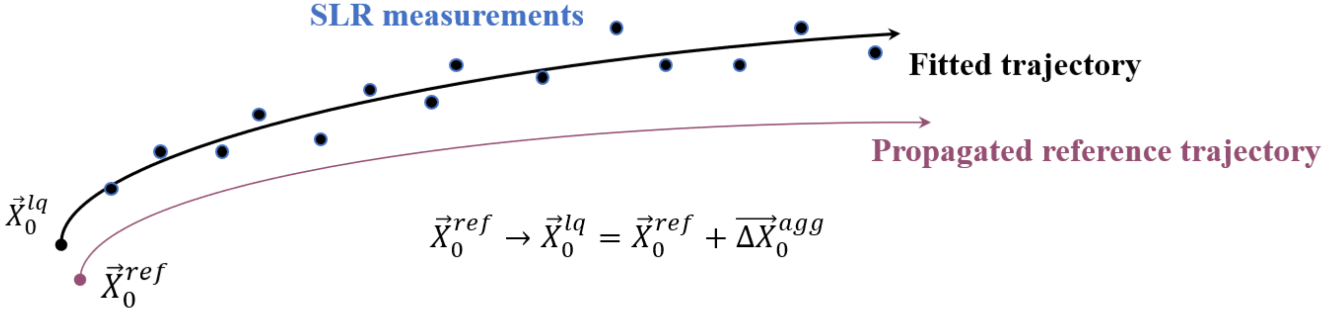

D. Lucchesi, G. Balmino, *The LAGEOS satellites orbital residuals determination and the Lense–Thirring effect measurement*. Plan. and Space Science, doi:10.1016/j.pss.2006.03.001 , **2006**

Precise Orbit Determination

POD and **models** for the two **LAGEOS** and **LARES** satellites:

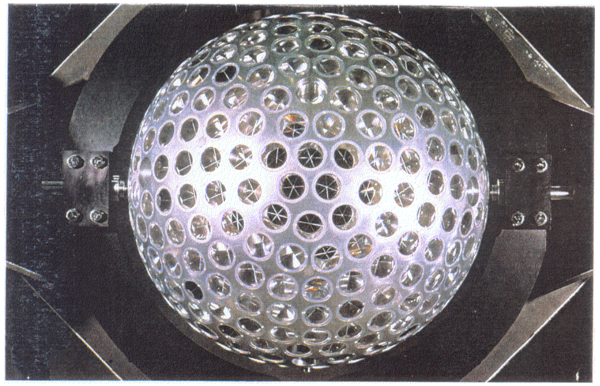

GEODYN II s/w

- Arc length, 7 days
- General Relativity: not modeled
- Empirical accelerations, CR, …: not estimated
- Non-gravitational perturbations: internal and external
- Gravity field: from GRACE and GRACE-FO solutions
- State-vector adjusted to best fit the tracking data
- …

TABLE III. Models currently used for the POD obtained from GEODYN II. The models are grouped in gravitational perturbations, non-gravitational perturbations and reference frames realizations.

Model for	Model type	Reference
Geopotential (static)	EIGEN-GRACE02S/GGM05S	[42–44]
Geopotential (time-varying: even zonal harmonics)	GRACE/GRACE FO	[43, 44]
Geopotential (time-varying: tides)	Ray GOT99.2	[45]
Geopotential (time-varying: non tidal)	IERS Conventions 2010	[41]
Third–body	JPL DE-403	[46]
Relativistic corrections	Parameterized post-Newtonian	[40, 47]
Direct solar radiation pressure	Cannonball	[38]
Earth albedo	Knocke-Rubincam	[48]
Earth-Yarkovsky	Rubincam	[49–51]
Neutral drag	JR-71/MSIS-86	[52, 53]
Spin	LASSOS	[54]
Stations position	ITRF2008/2014	[55, 56]
Ocean loading	Schernek and GOT99.2 tides	[38, 45]
Earth Rotation Parameters	IERS EOP C04	[57]
Nutation	IAU 2000	[58]
Precession	IAU 2000	[59]

Measurement and constraint

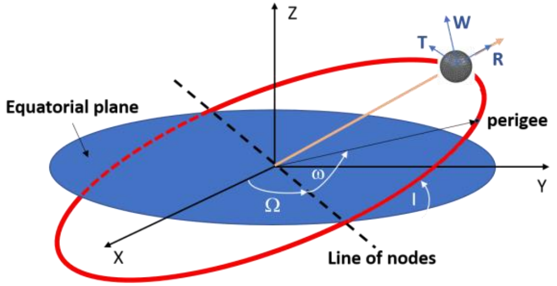

In our analysis:

- we concentrated upon the **yearly oscillation** of the **longitude** $(\omega + M)$ of the **LAGEOS II** satellite
- as **gravitationally preferred rest frame** we consider that of the **cosmic microwave background radiation**
- ***w*** represents the speed of the **Sun** with respect to this reference frame with orientation given by the following ecliptic coordinates $(\lambda_{PF}, \beta_{PF})$:

$$w = 368 \pm 2\ \frac{km}{s} \qquad \begin{cases} \lambda_{PF} = 171°.55 \\ \beta_{PF} = -11°.13 \end{cases}$$

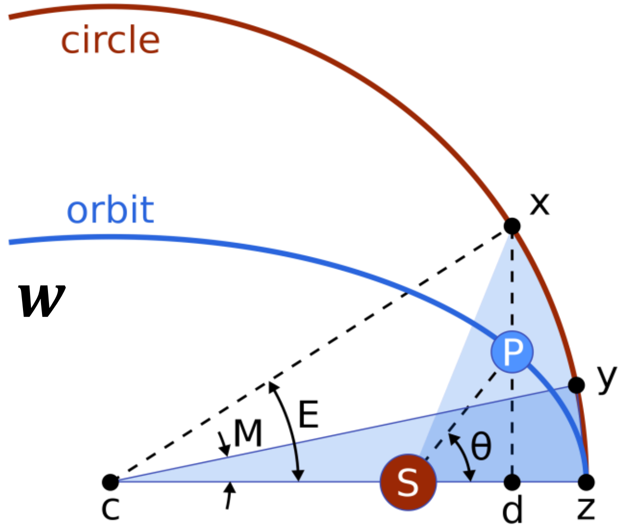

$$\mathcal{L}_{\alpha_1} = -\frac{\alpha_1}{4c^2} \sum_{a \neq b} \frac{G m_a m_b}{r_{ab}} \left(\boldsymbol{v}_a^0 \cdot \boldsymbol{v}_b^0\right) \qquad \boldsymbol{v}_s^0 = \boldsymbol{v}_s + \boldsymbol{v}_\oplus + \boldsymbol{w}$$

$$\mathcal{L}_{\alpha_1} = -\frac{\alpha_1}{2c^2} \frac{G M_\oplus m_s}{r_{\oplus s}} (\boldsymbol{v}_\oplus + \boldsymbol{w}) \cdot (\boldsymbol{v}_s + \boldsymbol{v}_\oplus + \boldsymbol{w})$$

Measurement and constraint

From **Lagrange's** perturbative equations we are able to extract the perturbative effect of a possible **PFE** on the **rate** of the **argument of pericenter** and on the **rate** of **the mean anomaly** of the satellite:

$$\frac{d\omega}{dt} = \frac{\sqrt{1-e^2}}{na^2e}\frac{\partial R}{\partial e} - \frac{\cot i}{na^2\sqrt{1-e^2}}\frac{\partial R}{\partial i}$$

$$\frac{dM}{dt} = -\frac{2}{na}\frac{\partial R}{\partial a} - \frac{1-e^2}{na^2e}\frac{\partial R}{\partial e}$$

R represents the perturbing funtion
$(a, e, i, \Omega, \omega, M)$ are the keplerian elements
n represents the satellite mean motion: $n = \sqrt{\frac{GM_\oplus}{a^3}}$

We finally obtain:

Earth mean motion:
annual frequency

$$\left(\dot{\omega} + \dot{M}\right)_{\alpha_1} = -\alpha_1 2n\frac{wv_\oplus}{c^2}\cos\beta_{PF}\sin(n_\oplus t - \lambda_{PF}) + \cdots$$

If **PFEs** exist, the quantity $\left(\dot{\omega} + \dot{M}\right)_{\alpha_1}$ must be present in the **residuals** of the two elements obtained from the **POD**.

Measurement and constraint

Procedure in the **time domain** to **extract** the **constraint** in the **PPN** parameter α_1:

1. Estimate from the **POD** the satellite **state-vector** for each **arc**
2. Obtain from the **state-vectors** the **residuals** in the **rate** of the orbital elements: $\dot{\omega}$ and $\dot{M}$
3. Build from these **residuals** the **gravitational observable**: $\dot{\omega} + \dot{M}$
4. Remove from the **observable** the **predictions** of the **unmodeled relativistic precessions**
5. Apply a **homodyne detection** to these data at the **expected frequency** (**the annual one**) for the effect described by the α_1 parameter and linked to the existence of the **PFE** due to the **cosmic microwave background radiation**
6. Apply a **low-pass filter** to the data
7. Calculate the **mean** from this last operation and from this **mean**, suitably renormalized, **extract** the value of the **PPN** parameter α_1

$$\left(\dot{\omega} + \dot{M}\right)_{\alpha_1} = -\alpha_1 2n \frac{w v_\oplus}{c^2} \cos\beta_{PF} \sin(n_\oplus t - \lambda_{PF}) + \cdots = \alpha_1 K \sin(n_\oplus t - \lambda_{PF}) + \cdots$$

$$K = -2n \frac{w v_\oplus}{c^2} \cos\beta_{PF}$$

Measurement and constraint

SaToR-G

Residuals in the two **observables** after the **POD**

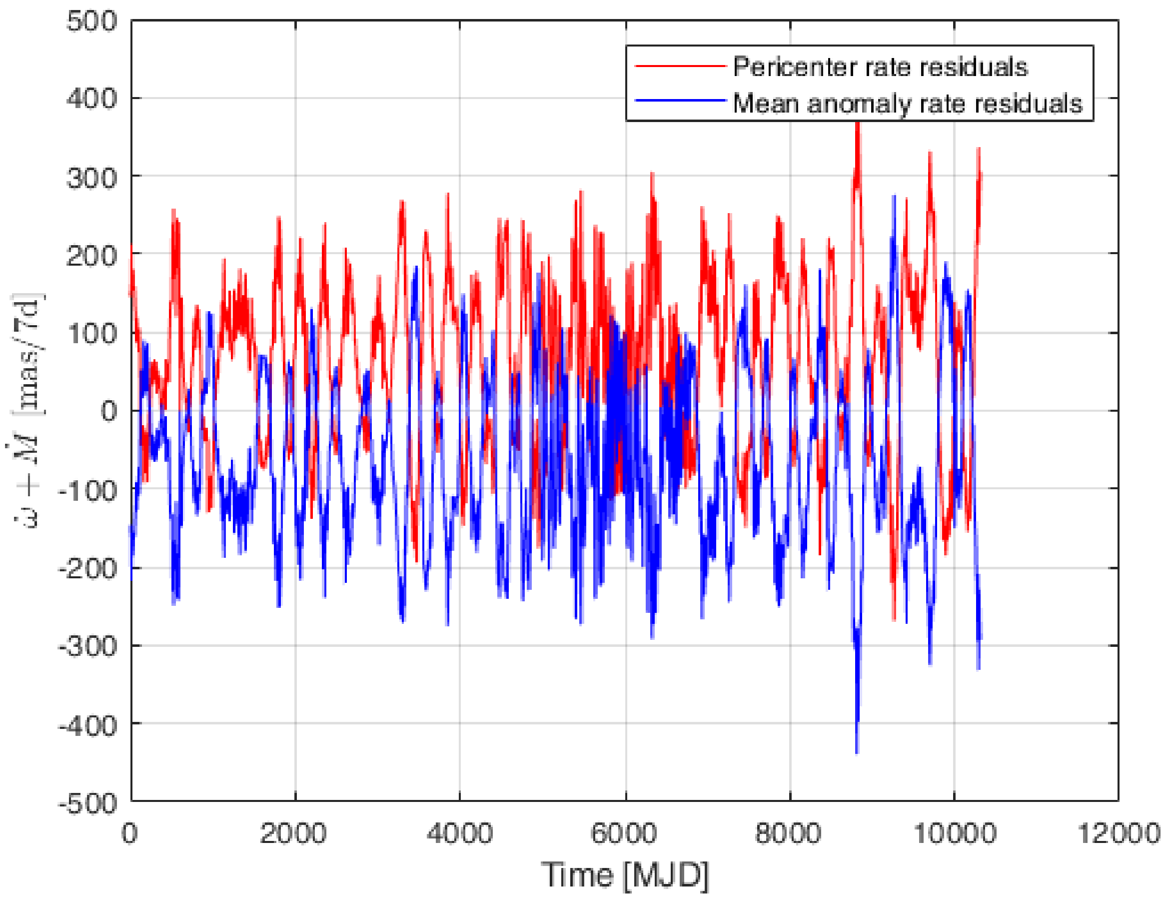

Relativistic precessions in the two **observables**

Rate (mas/yr)	LAGEOS	LAGEOS II	LARES
$\dot{\omega}_{Schw}$	+ 3270.78	+ 3352.58	+ 10,110.15
$\dot{\omega}_{LT}$	+ 31.23	– 57.33	– 124.53
$\dot{\omega}_{J2}^{dir}$	– 3.26	+ 2.85	– 23.38
$\dot{\omega}_{J2}^{indir}$	– 0.36	+ 0.16	– 2.65
Total	+ 3306.38	+ 3298.26	+ 9959.59
$\dot{M}_{Schw}$	– 3278.75	– 3352.26	– 10,110.14
$\dot{M}_{J_2 rel}$	– 0.92	+ 0.15	– 6.71
Total	– 3278.75	– 3352.11	– 10,116.85

$$\frac{d\omega}{dt} = \frac{\sqrt{1-e^2}}{na^2 e}\frac{\partial R}{\partial e} - \frac{\cot i}{na^2\sqrt{1-e^2}}\frac{\partial R}{\partial i}$$

$$\frac{dM}{dt} = -\frac{2}{na}\frac{\partial R}{\partial a} - \frac{1-e^2}{na^2 e}\frac{\partial R}{\partial e}$$

Measurement and constraint

<u>**Lock-in** analysis</u>

$$\left(\dot{\boldsymbol{\omega}}+\dot{\boldsymbol{M}}\right)_{\boldsymbol{\alpha}_1}=\boldsymbol{\alpha}_1\boldsymbol{K}\sin(\boldsymbol{n}_{\oplus}\boldsymbol{t}-\boldsymbol{\lambda}_{\boldsymbol{PF}})+\cdots \qquad \boldsymbol{K}=-2\boldsymbol{n}\frac{\boldsymbol{w}\boldsymbol{v}_{\oplus}}{\boldsymbol{c}^2}\boldsymbol{\cos\beta}_{\boldsymbol{PF}}$$

$$\sin(\boldsymbol{n}_{\oplus}\boldsymbol{t}-\boldsymbol{\lambda}_{\boldsymbol{PF}})\cdot\left(\dot{\omega}+\dot{M}\right)_{\boldsymbol{res}}=\alpha_1\,\mathrm{K}(\boldsymbol{sin}(\boldsymbol{n}_{\oplus}\boldsymbol{t}-\boldsymbol{\lambda}_{\boldsymbol{PF}}))^2+\cdots$$

Lock-in analysis, in this case more properly a **homodyne analysis** (**phase sensitive detection**), is mathematically based on **Werner's trigonometric formulas:**

$$\sin\alpha\sin\beta=\frac{1}{2}(\cos(\alpha-\beta)-\cos(\alpha+\beta))$$

$$\sin\alpha\cos\beta=\frac{1}{2}(\sin(\alpha-\beta)+\sin(\alpha+\beta))$$

$$\sin\alpha\sin\alpha=\frac{1}{2}(1-\cos(2\alpha))$$

If **α=β**, as in our case, a **part of the signal** goes in **continuous** (**DC**) and a **part** at **twice the annual frequency**.

Measurement and constraint

Analysis to fix the parameters of the low-pass filter:

- order
- integration time
- timespan for the averaging

Observable
Simulated data with no signal at annual frequency
Simulated signal with reference signal
Reference signal at annual frequency

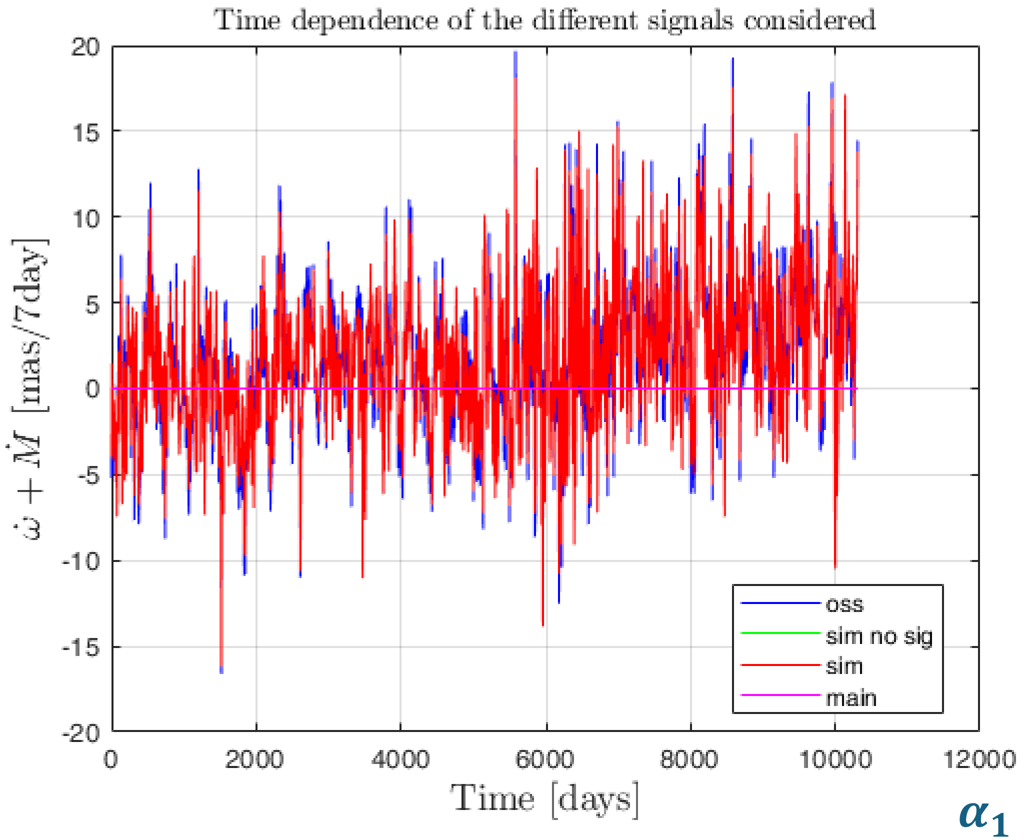

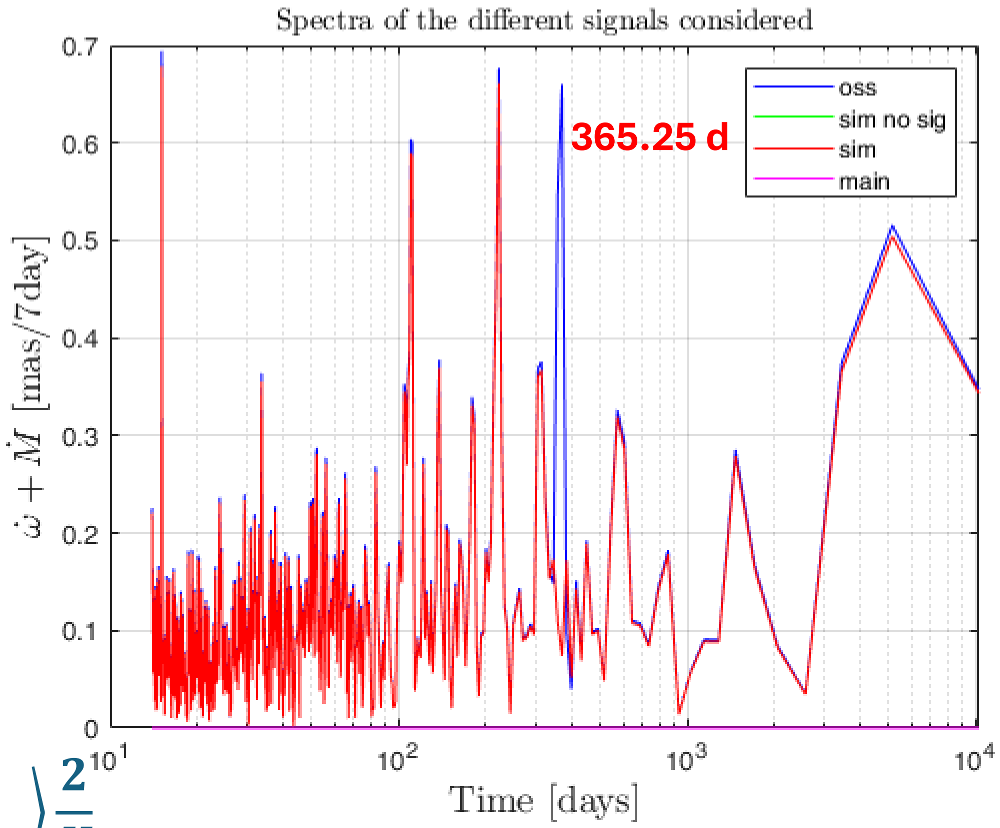

$$\alpha_1 = \left\langle \left(\dot{\omega} + \dot{M}\right)_{res} \right\rangle \frac{2}{K}$$

Measurement and constraint

Lock-in analysis:

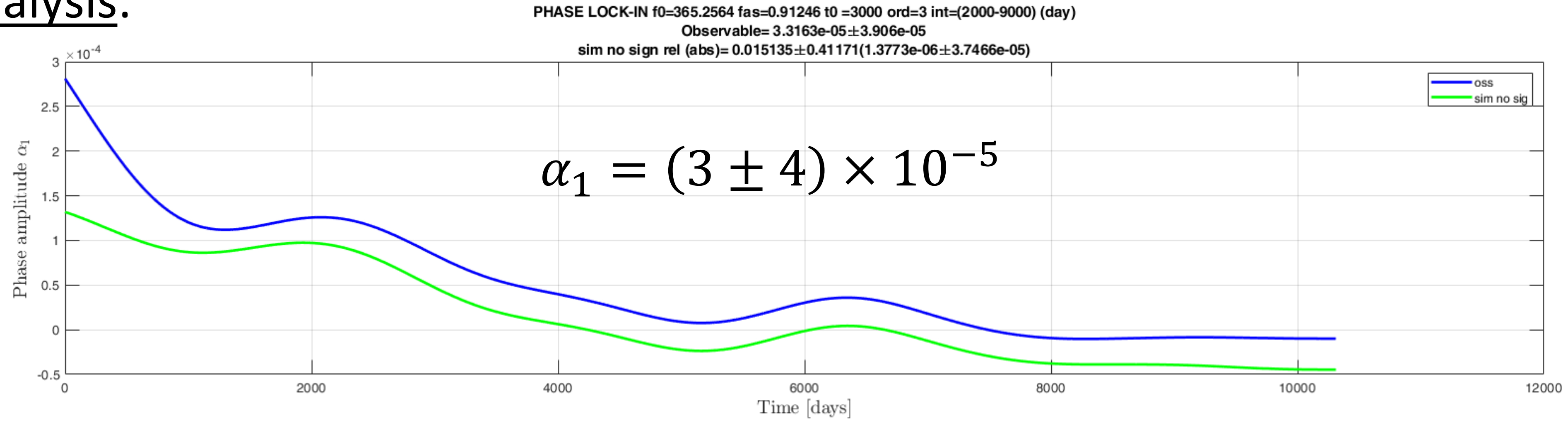

$$\alpha_1 = (3 \pm 4) \times 10^{-5}$$

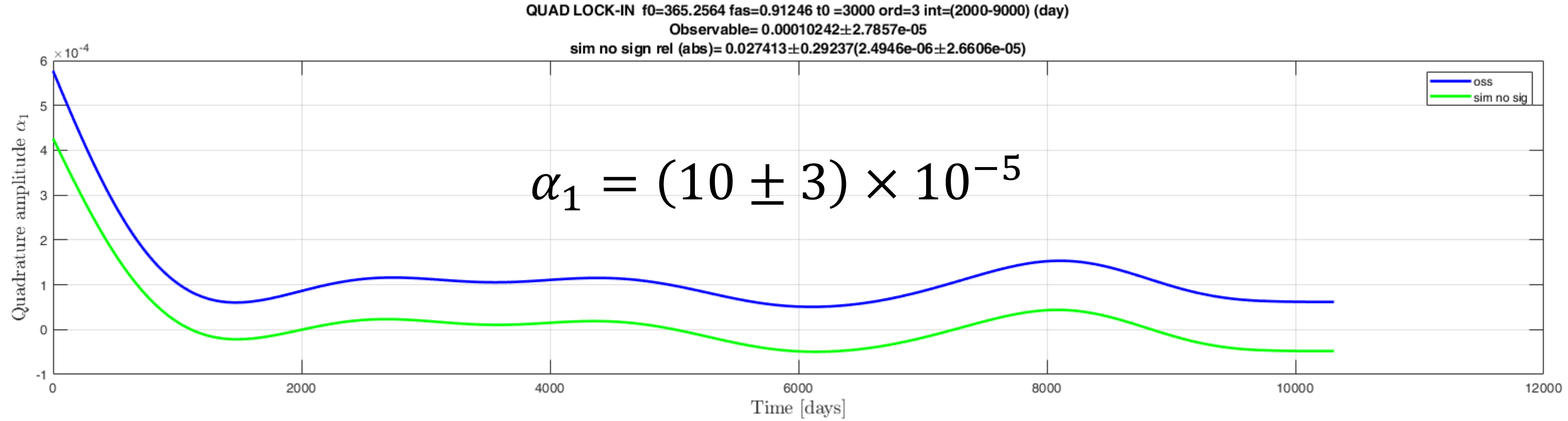

$$\alpha_1 = (10 \pm 3) \times 10^{-5}$$

Measurement and constraint

Scatter plot of the value of the **PPN parameter α_1** after the l**ock-in demodulation** as the **frequency** and signal **phase** vary and **α_1** behavior as a function of the phase.

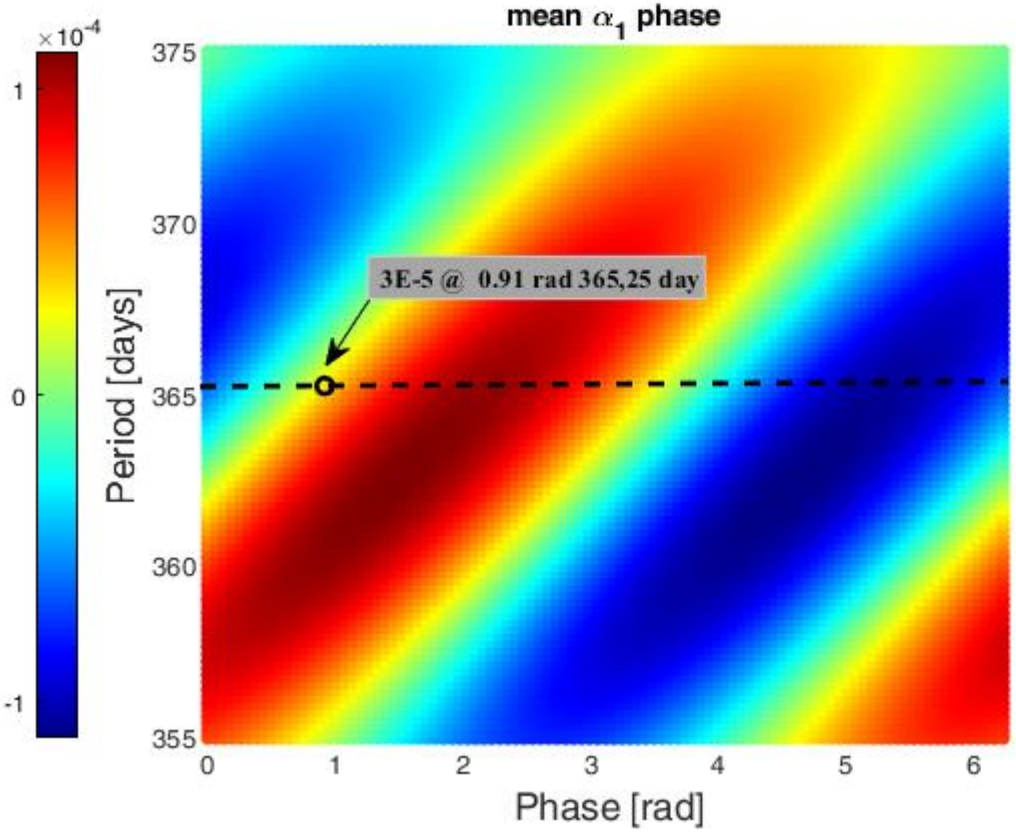

365.25 days signal

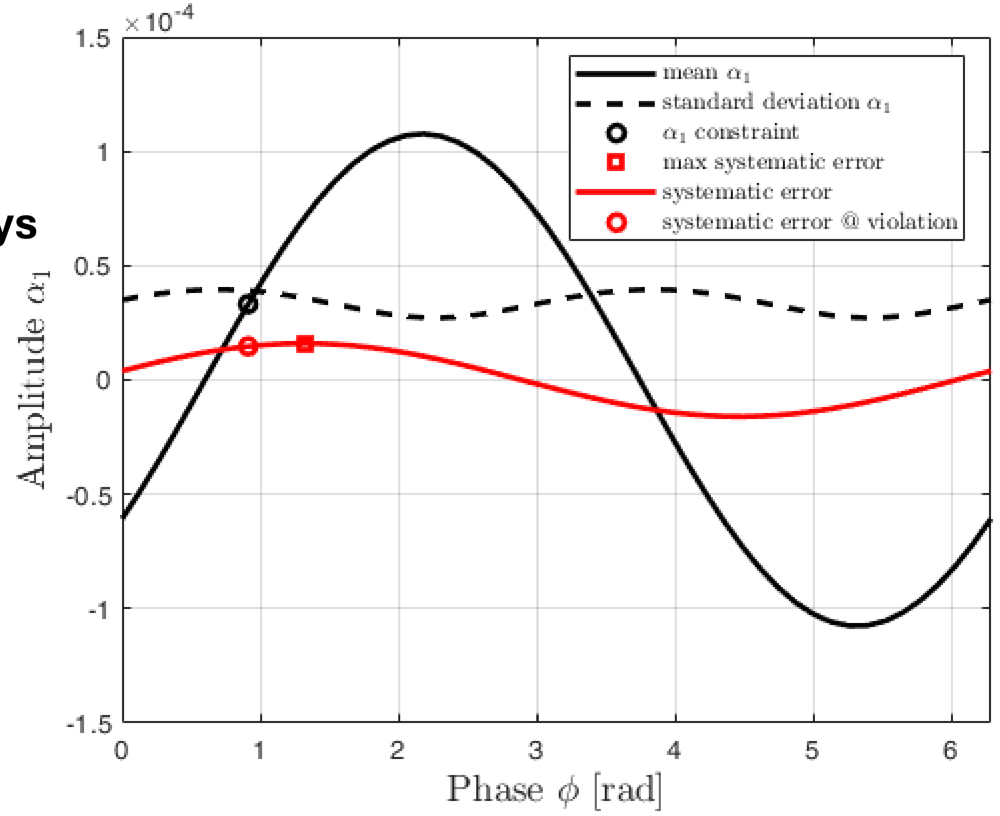

Measurement and constraint

Preliminary **error budget** for the **systematic errors**:

1. **Gravitational field (quadrupole)** $\delta\alpha_1 \cong 1.6 \times 10^{-5}$
2. **Solid tides** $\delta\alpha_1 < 9 \times 10^{-10}$
3. **Ocean tides** $\delta\alpha_1 \lesssim 2 \times 10^{-7}$
4. **Non-Gravitational Perturbations:** $\delta\alpha_1 \cong 0$

$$\delta\alpha_1 \cong 2 \times 10^{-5}$$

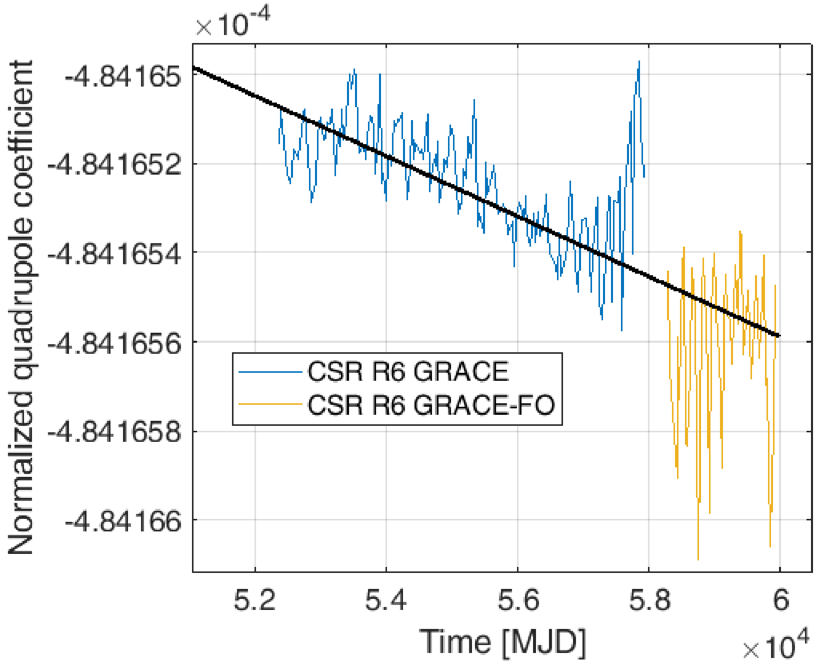

$$\delta(\dot{\omega} + \dot{M})\Big|_{\delta\bar{C}_{2,0}} \cong \frac{3}{2}\sqrt{5}\left(\frac{R_\oplus}{a}\right)^2 n(3 - 4\sin^2 i)\delta\bar{C}_{2,0}$$

$$\delta(\dot{\omega} + \dot{M})\Big|_{tide} \cong (\Delta\dot{\omega} + \Delta\dot{M})\cos\Phi\,\frac{\delta k}{k}$$

Tide 056.554	$\Delta\dot{\omega}$ (mas/d)	$\Delta\dot{M}$ (mas/d)	Φ
Solid	+ 0.0346	– 0.0128	+ 216°.17
Ocean	– 0.0745	+ 0.0276	+ 176°.82

Measurement and constraint

Result for the **PPN** parameter α_1 and constraint to alternative theories of gravitation:

$$\alpha_1 = (3 \pm 3) \times 10^{-5}$$

This result represents the **first constraint in α_1** in the **field** of the **Earth** based on a **pure gravitational experiment**.

The result obtained, although preliminary, confirms the validity of the **LLI** for gravitation and strongly constrains possible **PFEs** and, consequently, **vector-tensor theories of gravity**, at least in the **WFSM** limit of **GR**.

Measurement and constraint

SaToR-G

Comparison with the literature:

$\boxed{\alpha_1 = +3 \times 10^{-5} \pm 3 \times 10^{-5}}$ With **SLR** data from **LAGEOS II longitude**, 2023/2024

$\alpha_1 = -7 \times 10^{-5} \pm 9 \times 10^{-5}$ With **LLR** data from the **oscillations** of the **Earth-Moon distance**, 2008

$\hat{\alpha}_1 = -4 \times 10^{-6} \pm 4 \times 10^{-5}$ From **binary Pulsar** data, 2012

Müller J, Williams J G and Turyshev S G, 2008. Lunar laser ranging contributions to relativity and geodesy. *Lasers, Clocks and Drag-Free Control: Exploration of Relativistic Gravity in Space (Astrophysics and Space Science Library* vol 349*)* ed H Dittus, C Lammerzahl and S G Turyshev p 457.

J. Müller, K. Nordtvedt, D. Vokrouhlický, *Improved constraint on the α_1 PPN parameter from lunar motion*. Phys. Rev. D, Vol. 54, No 10, 1996.

L. Shao, N. Wex, *New tests of Local Lorentz invariance of gravity with small-eccentricity binary pulsars*. Class. Quantum Grav. 29, 2012.

Conclusions

- **Local Lorentz Invariance** represents one of the cornerstones of both the standard model of field and particle physics and the standard model of gravitation, i.e. of **GR**. In a sense, **LLI** represents our current deepest understanding of the nature of space and time. So, why test **LLI**?
- A strong motivation in our work is to search for the possible existence (or at least evidence) of **new physics** beyond **GR**. We mentioned the possible existence of additional fields that come into play in mediating the gravitational interaction and that could couple to matter in such a way, in some cases, that they violate Lorentz invariance.
- Therefore, in this work we have presented and discussed a test of **LLI**, and its possible violation, in the gravitational sector by exploiting the possible existence of **PFE**:

$$\alpha_1 = (3 \pm 3) \times 10^{-5}$$

The result is therefore fully compatible with zero, in agreement with GR

- The result we have obtained further constrains the possible existence of a preferred frame for local gravitational physics and, consequently, that of theories of gravitation described, in addition to the **metric tensor** of **GR**, by the presence of additional fields of **tensor** and/or **vector** nature.
- Consequently, this new result represents a first constraint on **LLI** through a **weak-field gravitation experiment** with a satellite orbiting the Earth.

The SaToR-G Team

@IAPS-INAF, Tor Vergata (RM)
- Marco Cinelli
- Alessandro Di Marco
- David Lucchesi
- Marco Lucente
- Carmelo Magnafico
- Roberto Peron
- Feliciana Sapio
- Massimo Visco

@Dept. Physics, Univ. Tor Vergata (RM)
- Massimo Bassan
- Giuseppe Pucacco

@ISTI-CNR, Pisa
- Luciano Anselmo
- Carmen Pardini

@IGN, Yebes (Spain)
- José Carlos Rodríguez

Back-up

Satellite Laser Ranging

The **geodetic** satellites are tracked with very high accuracy through the **Satellite Laser Ranging** (**SLR**) technique.

SLR allows to determine the **round–trip time** between **Earth–bound laser Stations** and **orbiting passive** (and non-**passive**) **satellites**.

The time series of range measurements are then a record of the motions of both the end points: the satellite and the station.

Thanks to the accurate modelling of both **gravitational** and **non–gravitational perturbations** on the orbit of these satellites, and considering a less than 1 cm **range accuracy**, we are able to determine their **Keplerian elements** with about the same **accuracy**.

The precision of the measurement depends mainly on the laser pulse width, about 1×10^{-10} s — 3×10^{-11} s

Matera (ASI-CGS)

Satellite Laser Ranging

The **ILRS** (**International Laser Ranging Service**) supports laser ranging measurements to **geodetic**, **remote sensing**, **navigation** and **experimental satellites** equipped with retroreflector arrays as well as to **reflectors** on the **Moon**.

ilrs.gsfc.nasa.gov

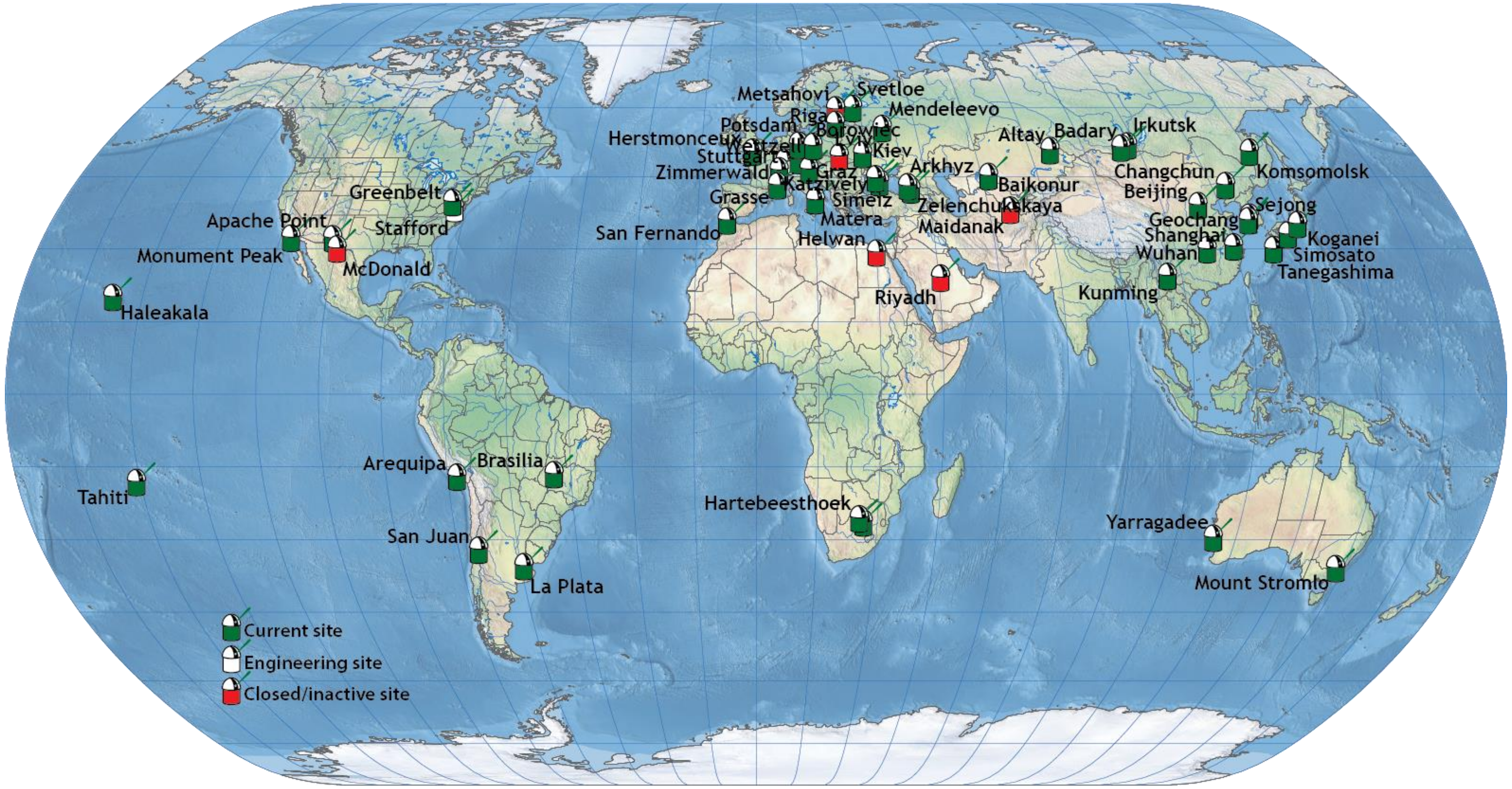

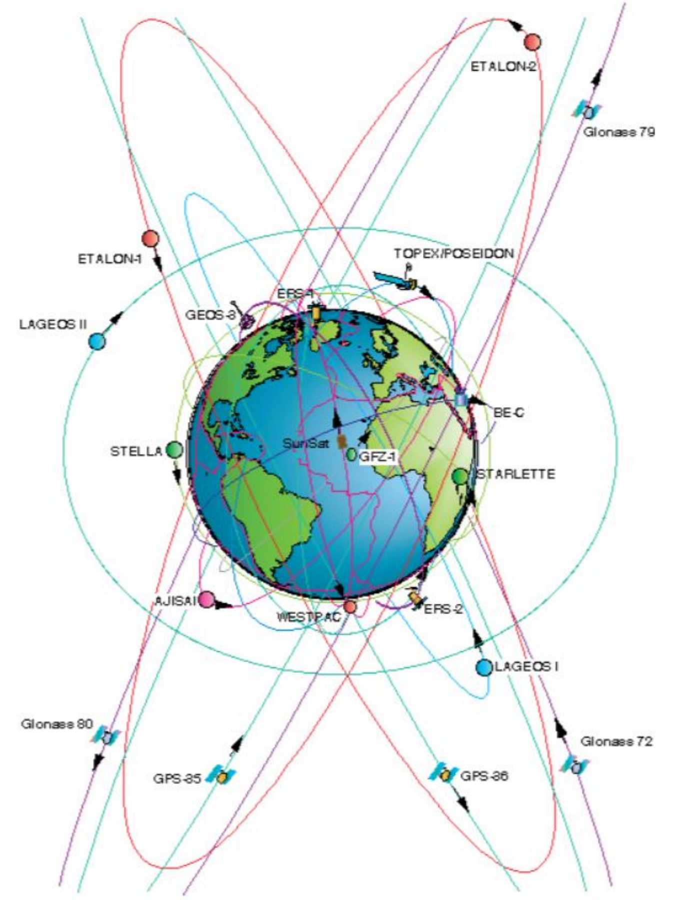

Precise Orbit Determination

Precise Orbit Determination (**POD**) has the **goal** of accurately determining the **position** and **velocity vectors** of an orbiting satellite.

To achieve this objective, **precise observations** of the satellite's **motion** and a **dynamic model** of the orbit as **accurate** as possible are necessary.

With these two ingredients it is possible to compute the **observable** to be **minimized** in a **least squares process**.

In the case of **SLR**, this **observable** is a **quadratic function** of the **range residuals *R***:

$$\boxed{\mathcal{R}_i = O_i - C_i}$$

Orbits:

$\frac{d}{dt}\vec{x} = f(\vec{x}, t, \vec{\alpha})$ Differential equation

$\begin{cases} \vec{x} \in \mathbb{R}^\ell \\ \vec{\alpha} \in \mathbb{R}^m \end{cases}$ State vector (position and velocity, …) / Models dynamic parameters (C_{20}, Cr, …)

$\vec{x}(t_0 = \vec{x}_0 \in \mathbb{R}^\ell)$ Initial condition at a given epoch: $\ell = 6 + \ldots$

$\vec{x} = \vec{x}(t, \vec{x}_0, \vec{\alpha})$ General solution for the orbits (*integral flow*)

Observations:

$C = C(\vec{x}, t, \vec{\beta})$ Observation function, $\vec{\beta} \in \mathbb{R}^n$ kinematic parameters

$$R_i = O_i - C_i = O_i - C(\vec{x}(t_i), t_i, \vec{\beta}) = \sum_j \frac{\partial C_i}{\partial P_j}\delta P_j + \delta O_i \qquad Q(\vec{R}) = \frac{1}{q}\vec{R}^T\vec{R} = \frac{1}{q}\sum_{i=1}^{q} R_i^2$$

Measurement and constraint

Residuals in the **observable** $\dot{\omega} + \dot{M}$

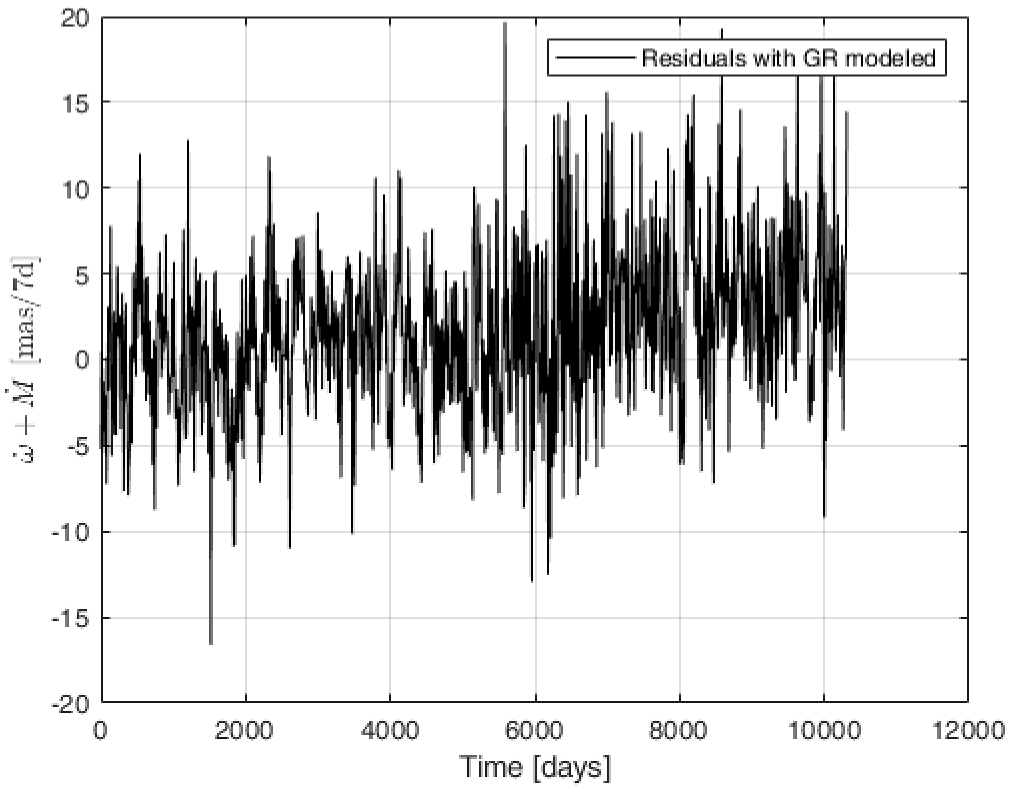

FFT of the **residuals** in the **observable**